Effect of a slit-shaped trap on depletion kinetics within a microchannel

Sung Hyun Park,[1] Hailin Peng,[1] Raoul Kopelman,[1,*] Panos Argyrakis,[1,2] and Haim Taitelbaum[3,*]
[1]*Department of Chemistry, University of Michigan, Ann Arbor, Michigan 48109-1055, USA*
[2]*Department of Physics, University of Thessaloniki, 54124 Thessaloniki, Greece*
[3]*Department of Physics, Bar-Ilan University, Ramat-Gan 52900, Israel*
(Received 29 July 2005; revised manuscript received 24 January 2006; published 27 April 2006)

The diffusion-limited trapping reaction kinetics of the growth of the depletion zone within and around a "slit-shaped" trap in a flat microchannel was studied experimentally and numerically. In the experiment, an ellipse-shaped laser beam acted as a slit trap in a long, flat capillary, and the trapping reaction is photobleaching of fluorescein dye. The parameter studied was the θ distance, i.e., the distance from the trap to the point where the reactant concentration has been locally depleted to the specific survival fraction $[\theta]$ of its initial bulk value. When the trap is perfect, then, due to the geometry of the trap and the reactor, as many as three time regimes can be found, with up to two crossover transitions. The number of crossovers is determined by the relative sizes of the trap and the microreactor. In the case of two crossovers, we show that the first crossover relates to the length of the trap, while the second crossover relates to the width of the reactor. When the slit trap is imperfect and its width cannot be neglected, as is the case in the experiments, a nontrivial early behavior is observed, followed by two regions in time, separated by a single crossover only.

DOI: 10.1103/PhysRevE.73.041104 PACS number(s): 82.50.−m, 82.20.−w, 05.40.Jc

I. INTRODUCTION

During the past two decades, diffusion-limited reaction kinetics have drawn much attention, as it has been noticed that the conventional kinetics laws do not apply to diffusion-limited reactions in low-dimensional [less than three-dimensional (3D)] environments [1–4]. A low dimensionality of a reactor hinders the effective diffusional (and/or convectional) mixing of the reactants, and this inefficiency results in the formation of reactant domains, where one reactant species is dominant in one local domain while another reactant is dominant in another local domain. Additionally, different space restrictions in different directions give rise to various dimensional crossovers [5–7]. The end effect is to slow down the overall reaction rate, albeit in a complicated way.

Among several reaction models, the trapping reaction $A+T\rightarrow T$ is one that draws much interest, due to its simplicity and wide application to a variety of problems [4]. For example, the kinetics of the trapped particles is an analogue of the case of ions around an electrode, which has been extensively studied during the 1960s [8–12]. In a typical model, T is a static trap and A is a diffusing species which is annihilated, with a certain probability, upon its collision with the trap. A dynamic "self-segregation" zone (a depletion zone) forms around the trap where the diffusive reactants A are depleted. The kinetics of this depletion zone in lower dimensions is different from the kinetics in a 3D environment. This can be experimentally studied by reactors of different shapes which reflect different dimensionalities.

Prior to this work, we explored the growth of a depletion zone in several environments: a line trap in a two-dimensional (2D) reactor [giving an effective one dimensional (1D) behavior] [13], a point trap in a 2D reactor [14,15], and a point trap in a flat capillary [16]. The present work is an extension to the latter, in order to further explore the ramifications from the sensitivity of the diffusion-limited reaction kinetics to the geometry of the reactor and the trap. As in our previous studies, we follow the quantity called the θ distance, r_θ, defined as the distance from the trap to the point where the local concentration is a fraction, θ, of the bulk concentration. We discuss how r_θ scales with time, noting that this parameter is easier to obtain experimentally than other quantities, such as, e.g., the so-called nearest-neighbor distance [17,18], which has to do with the discrete nature of the particles. Formally, r_θ is defined as

$$c(r_\theta,t)=\theta c_0, \tag{1}$$

where $c(r,t)$ is the concentration of A particles at distance r at time t, starting from an initial concentration c_0 at time $t=0$.

In 1D systems, the θ distance has been found to increase as $t^{1/2}$ asymptotically by experiments and theory [13]. This result can be understood in terms of the simple Einstein diffusion. In 2D, however, it is observed that the θ distance increases nonuniversally, scaling as $t^{\theta/2}$ in the long-time limit, i.e., its time behavior depends on the arbitrary fraction θ [14,15,19–21]. The slower growth of the depletion zone in the 2D systems, compared with the 1D systems, is explained as being due to the more effective mixing in 2D systems. In 3D systems the depletion zone does not grow at all, as the diffusional mixing is most effective.

In this paper, a flat, rectangular capillary is used with a laser beam forming a slit (instead of a point) shape therein. A schematic figure of the system is shown in Fig. 1. This system differs from the previous 1D system (a line trap in a 2D lattice [13]) in that the reactor is narrower and also bounded, and the line trap does not span over the entire width of the reactor. As expected from previous studies using a capillary

*Authors to whom correspondence should be addressed.

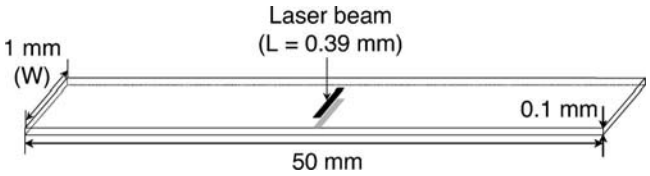

FIG. 1. Schematic graph of the experimental setup. A line-shaped trap is located in a rectangular shape reactor.

system [16], one can again observe dimensional crossover transitions. However, in the present system, *two* crossover transitions are expected, the first from a 1D behavior to a 2D behavior, when the depletion zone expands from the center of the trap to the ends of the trap, and the second is back from a 2D behavior to a 1D behavior, as the depletion zone expands beyond the ends of the trap and reaches the inner boundary of the reactor. These crossovers are nontrivial, as they reflect the change of the depletion zone kinetics from universal to nonuniversal behavior and back. We show that this is indeed the case for a *perfect* trap. The effects of the slit shape, i.e., the finite length of the *trap*, are significant only at very early times, but insignificant at longer times, where the behavior is the same as for a point trap. Similarly, our results show that the effects of the finite size of the *reactor* are significant only at longer times, but insignificant at earlier times. However, for the case of an *imperfect* trap, as is the case in the experiments, we obtain a nontrivial behavior at early times, followed by two time regions (2D, 1D) with a single crossover in between. This is similar to the results for a point trap in a flat microchannel [16].

II. MICROCHANNEL EXPERIMENTS

A. Experiment

The experiment is the photobleaching reaction of fluorescein dye molecules in an aqueous solution by a focused laser beam. The reactor is a flat, rectangular capillary and its dimensions are 50 mm $\times$ 1 mm $\times$ 0.1 mm. Figure 1 shows a schematic graph of the reactor and the trap we used. An aqueous solution of fluorescein (concentration 3.6×10^{-5} M) was injected into the reactor and the openings of the reactor were sealed using epoxy after the injection.

Two kinds of light sources are used in the experiments: a laser beam as the source of the trap and another beam as a probe. A blue laser light (488 nm) from an argon ion laser was expanded to an approximately 2.5 cm diameter, using two biconvex lenses and then focused to a line shape by a cylindrical lens ($f=15$ cm). The power of the laser beam is about 10 mW. The probe beam was from a xenon lamp coupled with a 480 nm bandpass filter. The laser beam comes to the top of the reaction chamber and the probe beam to the bottom. The shape of the laser beam on the capillary is an ellipse and the lengths of the major and minor axes are 0.39 mm and 0.15 mm, respectively. Since the minor axis is much smaller than the major one, we regard the shape as a slit. The laser beam from above the capillary was introduced in such a way that it lies perpendicular to the longer boundary of the capillary and the two ends of the major axis of the ellipse have the same distance to the two longer boundaries of the capillary, as schematically shown in Fig. 1.

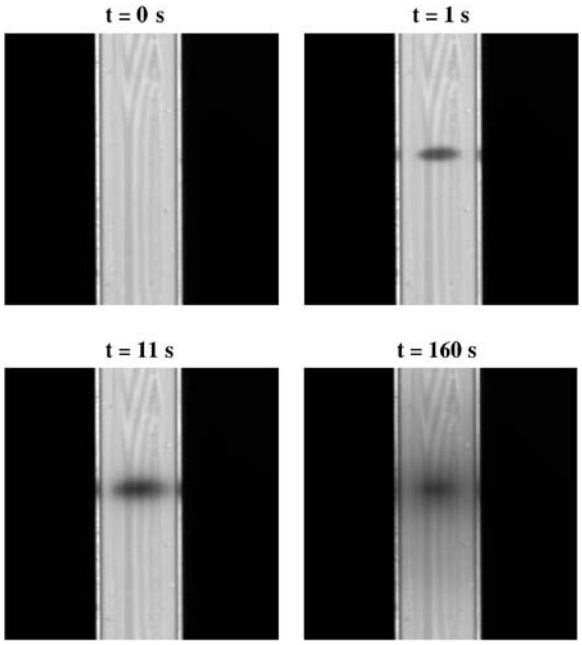

FIG. 2. The fluorescence image before the photobleaching reaction begins and selected fluorescence images ($t=1$, 11, and 160 s) after the photobleaching reaction starts.

We collected the fluorescence images by using a CCD camera (Roper Scientific, Photometrics Coolsnap ES) equipped with a macro lens (Nikon, AF Macro 60 mm f2.8, 1:1). The size of a typical image is 4.5×3.3 mm^2, or 695 $\times$ 518 pixels, with 14-bit intensity resolution. The resolution of a pixel is about 6.5 μm, so that the slit trap axes are 60 and 23 pixels. The dye molecule becomes invisible to the detector when photobleached, resulting in the intensity drop in the fluorescence image. The progress of the photobleaching was monitored up to 1900 s in the typical experiment. The entire experiment is performed at room temperature. A similar experimental setup has been used recently to study similar trapping reactions [13–16].

B. Results and discussion

Figure 2 shows the fluorescence image before the trapping reaction starts ($t=0$) and several selected fluorescence images after the trapping reaction starts, at $t=1$, 11, and 160 s, illustrating the progress of the photobleaching reaction. The bright vertical bands in the middle of the images represent the flat rectangular capillary, or the reaction channel. The dark region within the reactor, growing with time, is the depletion zone produced by the photobleaching reaction. No evidence for convection was seen. The depletion zone resembles the trap shape at $t=1$ s in Fig. 2. Unlike the depletion zone around a point trap in pure 2D, the depletion zone created by a slit trap is obviously not radially symmetrical. The concentration profiles along the pixel line that is parallel with the reaction channel and crosses the center of the slit trap are the simplest ones. They are denoted as $C_{\|}$, as in the

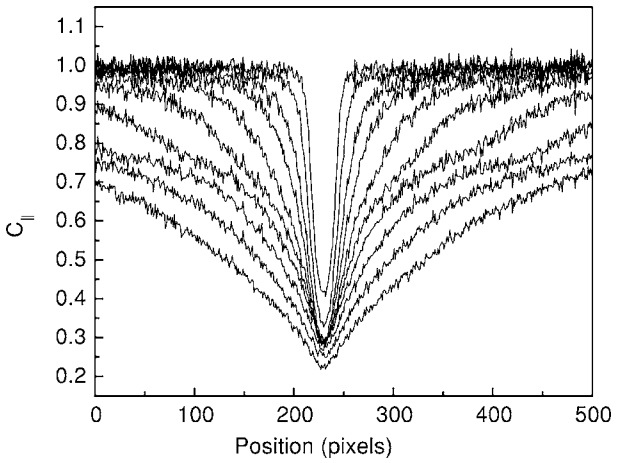

FIG. 3. Experimental data of the concentration profile at different times. The laser power is 10 mW, which is considered as an imperfect trap. The times are 2, 5, 14, 25, 50, 130, 260, 500, 980, 1900 s (top to bottom).

work on the point trap in a slab geometry [16].

Figure 3 shows the time evolution of these profiles. The time range is from $t=1$ to 1900 s. Before the depletion zone reaches a certain location, the concentration at that location is the bulk concentration. When the relative concentration at the boundary is less than the initial bulk concentration, it means that the depletion zone has reached the boundary, as is the case, e.g., in Fig. 2(d), which is the fluorescence image at $t=160$ s.

Each θ distance at a given time is measured from the corresponding concentration profile and presented in Fig. 4(a) as a function of time. The solid line in the figure has a slope of 1/2, corresponding to the theoretical $t^{1/2}$ behavior in 1D, and the dotted lines have slopes of $\theta/2$, corresponding to the theoretical $t^{\theta/2}$ in 2D. It can be seen that the θ distance approaches a $t^{1/2}$ slope asymptotically, as is reconfirmed in Fig. 4(b), where we show that $r_\theta/t^{1/2}$ tends to a constant asymptotically. The somewhat higher slope for $\theta=0.8, 0.9$ resembles a similar behavior found for a point trap inside a microchannel [16]. It should eventually converge to the asymptotic 1/2 slope, as is indicated by the pattern of the curves for these values of θ in Fig. 4(b), which resembles the convergence trend for $\theta=0.7$ in this figure.

Prior to the asymptotic behavior, the θ distances scale differently for different θ values, i.e., as $t^{\theta/2}$. This is as expected: before the rectangular reactor constraint (the reactor shape) is fully "recognized" by the depletion zone, the θ distance scales as if the system was in an unbounded 2D plane. After the rectangular reactor constraint is fully "recognized," the θ distance scales with a 1D behavior.

We also notice that before the θ distance displays a 2D behavior, one may expect a period when the θ distance is showing a 1D behavior, but we do not see it here from our experimental results. Rather, we see an early time behavior with a growth *faster* than the 1D behavior for small θ, and a growth *slower* than 1D for large θ. Based on previous work [13–16], we suspect that this is due to the imperfectness of the trap in our experiments. The early time behavior resulting from the imperfect trapping prevents one from observing the first 1D regime experimentally. Thus, we simulate an imperfect trap (as well as a perfect trap) using the exact enumeration method.

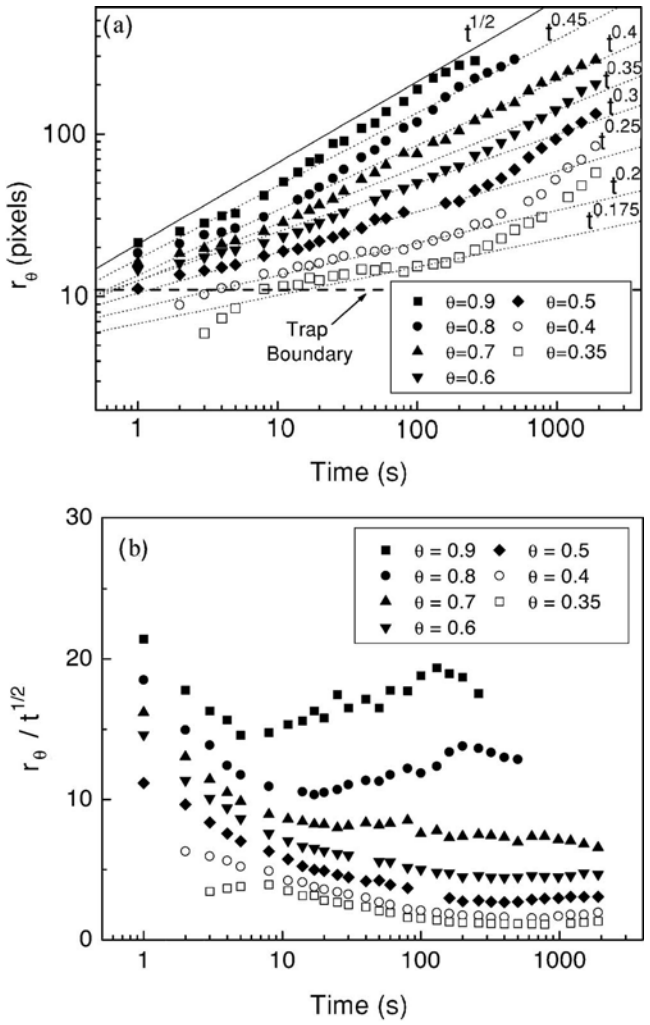

FIG. 4. (a) The θ distance plots (pixels) vs time (seconds) at different θ's for the experimental data of Fig. 3. (b) The data of (a), where the θ distance is divided by $t^{1/2}$. The asymptotic tendency to a constant confirms the 1D behavior of the third regime.

III. NUMERICAL CALCULATIONS

A. The exact enumeration method

Exact enumeration (EE) calculations are performed on a sufficiently long rectangular lattice of width W, with a slit trap of length L. The trap width (parallel to the long dimension of the capillary) is either a single lattice unit or more. The trap lies in the middle of the lattice and is perpendicular to the long edges of the rectangular lattice (see Fig. 1 for a schematic). The EE method is a discretisation of the diffusion equation for the concentration [22]. The initial bulk concentration is 0.25, including inside the trap. At each time step, the concentration at one site is equally divided and distributed to its four neighbors and, at the same time, the site accepts the concentration flow from all of its four neigh-

bors, each contributing 1/4 of the concentration at the previous time step. Before the depletion zone reaches a site, the concentration at this site is the bulk concentration. The boundary condition is reflective at the long edges of the rectangular lattice and cyclic at the short ones.

At the trapping zone, we assign a trapping probability (strength) p between 0 (no trapping) and 1 (perfect trap) to each trapping site. Traps with trapping probability greater than 0 but less than 1 are called imperfect traps. At every time step, a portion p of the flux entering the trapping zone is eliminated, while the remaining $1-p$ is "reflected" backwards into the bulk.

We note that we have also performed Monte Carlo simulations and the results were essentially the same.

B. Results and discussion

Imperfect trap

The imperfect trap corresponds to the experimental system in the sense that the laser power is finite. We have discussed in [14] how one can estimate the relative trapping efficiency from the laser power output. Figure 5(a) shows the results for an imperfect trap with trapping probability 0.5. The width of the reactor (W) is 11 lattice units and the length of the trap (L) is 5 lattice units. In order to mimic the slit trap in the experiment, the trap has a width of 3 lattice units, so it is actually a rectangular rather than an ideal slit. In Fig. 5(a) the θ distance shows the behavior of 2D and 1D at intermediate and long times, respectively. At early times, the θ distance does not show the 1D behavior, which is expected for the perfect trap case, but rather rises either faster than $t^{1/2}$ for small θ, or slower than $t^{1/2}$ for large θ, similar to the experimental results. This supports the contention that the trap in our experiment is not a perfect trap.

Figure 5(b) shows $r_\theta/t^{1/2}$ vs time for the same data as in Fig. 5(a). The $r_\theta/t^{1/2}$ data show a clear tendency to converge to a constant at long time limit, which supports our earlier argument that the higher slope for $\theta=0.8$ and 0.9 in Fig. 4(b) should eventually converge to the asymptotic 1/2 slope.

Perfect trap

Figure 6 shows the θ distance vs time for an ideal perfect slit trap (trapping probability = 1) from EE calculations. The width of the reactor (W) is 25 lattice units and the length of the trap (L) is 5 lattice units. Its width is a single lattice unit. We added several short lines to be able to identify slopes of 1/2 (solid lines) and slopes $\theta/2$ (dotted lines). We observe both the 2D and 1D behavior in the figure. Take $\theta=0.8$ as an example: At the earliest times, the θ distance scales as $t^{1/2}$, a 1D behavior, then it scales as $t^{\theta/2}$ between 10 and 200 time steps, and finally it crosses over to $t^{1/2}$ after $t=200$ time steps. If we follow our reasoning, at the very beginning the depletion zone has yet to "escape" from the effect of the symmetry of the trap, which acts as a quasi-1D system, as the line trap does in a 2D lattice [13].

As expected, there exist three distinct time regimes in the perfect slit trap system embedded inside a slab geometry. In the first regime, when the concentration along the middle line across the trap has not yet been affected by the finite size of the trap, the θ distance scales as $t^{1/2}$ as in 1D. In the second regime, when the effect of the finiteness of the trap on the concentration along the middle line has started but the finiteness of the reactor has not yet affected the concentration along the middle line, the θ distance scales as $t^{\theta/2}$, as in 2D; finally, in the third regime, when the finiteness of the reactor takes effect, the θ distance scales as $t^{1/2}$ again. This three-regime behavior is due to both the shape of the trap and that of the reactor, and gives rise to two crossover times.

We study the behavior of the first crossover time by fixing the width of the reactor while changing the length of the trap. Figure 7(a) shows the θ distance vs time at a fixed $\theta=0.6$, where W is fixed at 25 lattice units while L changes from 1 to 25 lattice units. From Fig. 7(a), we learn that the smaller the trap is, the earlier the first crossover time occurs. This is understandable, since, as explained earlier, the crossover

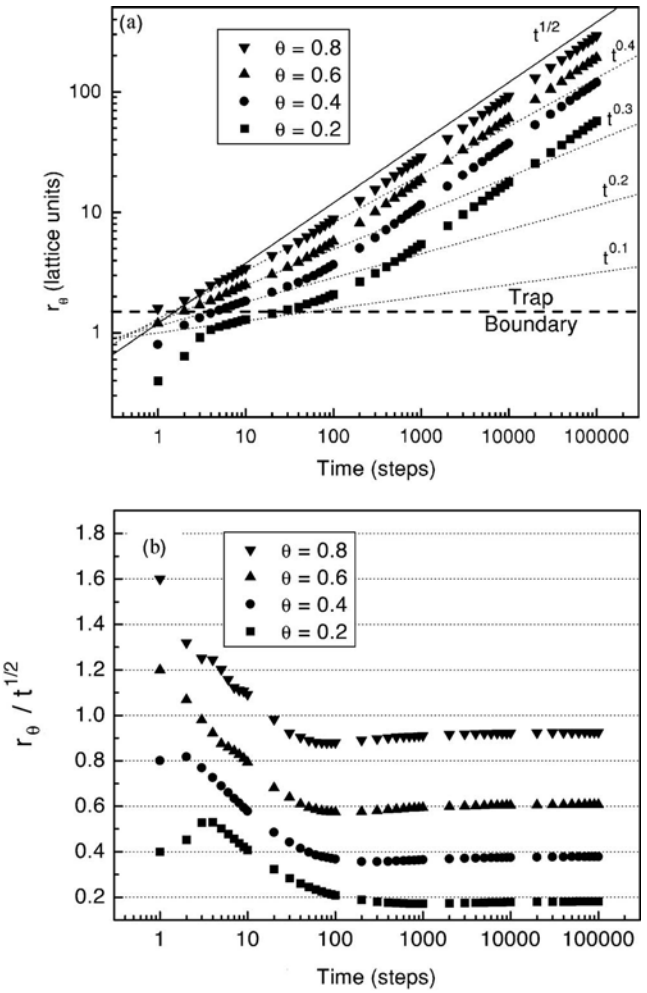

FIG. 5. (a) EE data of θ distance vs time (steps) for an imperfect trap ($p=0.5$). The reactor width is $W=11$ and the slit is $L=5$ lattice units in length perpendicular to the microchannel, and 3 lattice units in width in the parallel direction, in order to mimic the laser beam finite size. Similar to the experimental data, the three regimes are obtained: An early-time behavior (faster than $t^{1/2}$ for small θ and slower than $t^{1/2}$ behavior for larger θ), then a 2D behavior, and finally a 1D behavior. (*b*) $r_\theta/t^{1/2}$ vs time for the data of (a). The $r_\theta/t^{1/2}$ tends to converge to a constant at the long time limit.

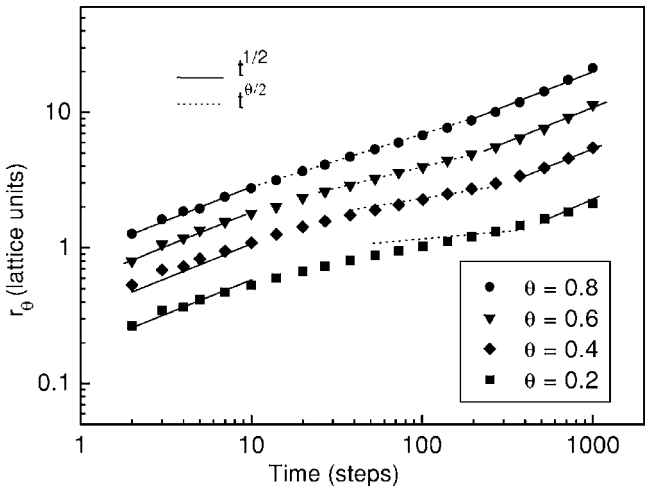

FIG. 6. EE data of θ distance vs time for a perfect trap at different θs. Three time regimes can be seen: 1D behavior ($t^{1/2}$), then 2D behavior ($t^{\theta/2}$), and finally 1D behavior ($t^{1/2}$).

transition occurs when the finiteness of the trap affects the concentration of the middle line, and this effect will take place earlier if the trap is smaller. The two possible limits of the ratio L/W can be inferred from Fig. 7(a). If we look at the data set for the trap length $L=1$, we recover the limit of a point trap in a slab, with essentially one crossover from 2D to 1D (see Ref. [16]). If we look at the $L=25$ data set ($L=W$), we recover the limit of the line trap which exhibits a 1D behavior with no crossovers at all [13]. We can determine the first crossover time by using this data set as the baseline. We compare each data set with it and record the time when the difference is 5%. We also assume that the crossover time change between any two discrete data points is linear and we can pick the time within the range of two points where the corresponding r_θ of one point has a difference less than 5% and the corresponding r_θ of the other has a difference more than 5% compared with the baseline. We plot the first crossover time vs L in a log-log plot in Fig. 8 (as filled squares). It can be seen that, apart from the limit of small L where the trap shape is actually a point, there is a square dependence of the first crossover time on the trap length, as is indicated by the solid line of slope 2.

In order to study the behavior of the second crossover time, we fix L and change W. Figure 7(b) shows such a plot where L is fixed at 5 while W varies from 15 to 51. Similar to the first crossover time, the second crossover time occurs earlier with a narrower reactor. We take the case of $W=51$ and $L=5$ as the baseline and record the time when the difference is 5%, by picking the time between two points as we picked the first crossover time. We plot the second crossover time vs W in a log-log plot in Fig. 8 (as circles). The slope is again around 2.

As we explained so far, the appearance of the three regimes is determined by the shape of the trap and the reactor. The shape of the trap makes the second regime (2D behavior) appear, while the *length* of the trap determines *when* it appears, i.e., the first crossover; the shape of the reactor makes the third regime (1D behavior at very long time) appear, while the *width* of the reactor determines *when* it ap-

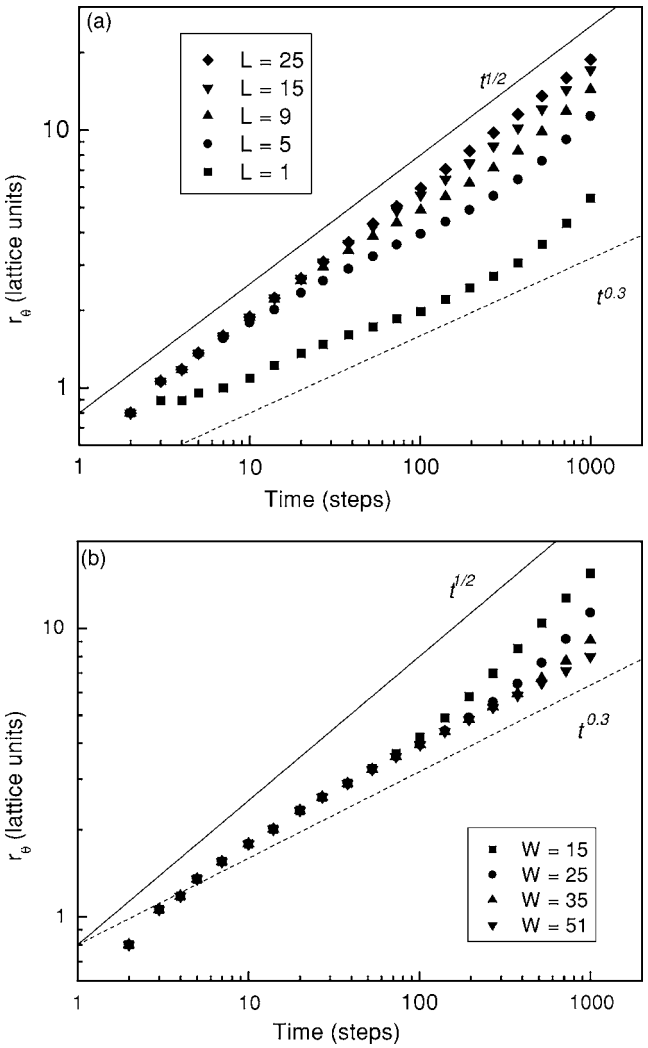

FIG. 7. EE data of θ distance vs time for a perfect trap at $\theta=0.6$. (a) Fixed reactor width ($W=25$), and different lengths of traps. The baseline ($W=25, L=25$) is at the top and only has 1D behavior. Other lines deviate from this line at different times, with smaller traps deviating first. (b) Fixed trap length ($L=5$) and different widths of reactors. The baseline ($W=51, L=5$) is at the bottom. Other lines deviate from this line at different times, with smaller reactors deviating first.

pears, i.e., the second crossover. Although the intermediate region exhibits a *nonuniversal* 2D behavior, we assume that the effects of the shapes of the trap and the reactor are still controlled by diffusion. This means that we expect Einstein's diffusion law, $L \sim t^{1/2}$ to be valid, and the crossover time τ to follow an L^2 behavior. Our results confirm this conjecture.

In terms of theoretical analysis, the current system involves a combination of two solvable systems: A line trap in 2D free space, and a point trap in a 2D constrained slab geometry. The first one is known to behave as an effective 1D trap with respect to the kinetics along the parallel direction [13]. In Ref. [16] we solved analytically the second case. However, it seems that the current system cannot be solved analytically, since we have a combination of two spatial parameters, each imposing difficulties on the exact solution: the trap length and the reactor width. Moreover, since the trap

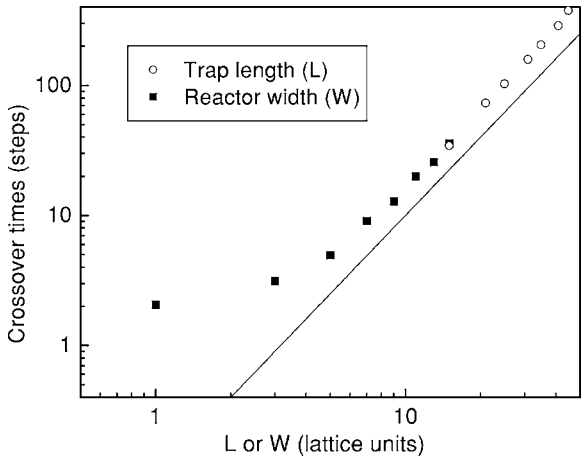

FIG. 8. The first crossover time vs trap length (L) for a fixed reactor width at $W=25$ (squares), and the second crossover time vs reactor width (W) for a fixed trap length at $L=5$ (circles) for perfect traps. The solid line is a slope of 2.

acts continuously in time, one needs to integrate over time. This makes things even more complicated and intractable. In any case, the insight gained from the two basic systems allows us to predict the behavior of the current system. This must depend on the ratio L/W of the trap length and the slab width. We claim that this ratio determines the number of crossovers in the kinetic behavior. When $L/W \to 0$, we have an effective point trap and one crossover (from 2D to 1D) is expected, as in Ref. [16]. When $L/W \to 1$, we have a 2D line trap extending throughout the reactor. The kinetic behavior along the parallel direction is 1D for all times, with no crossovers at all. When L/W is equal to some finite number between 0 and 1, then we expect two crossovers: 1D-2D-1D, as explained in detail above. In this case, the first crossover depends on the smaller length scale, L, while the second one depends on the larger length, W, as can be seen in Figs. 7(a), 7(b), and 8.

IV. SUMMARY

We treated the problem of the kinetics of the growth of a depletion zone around a slit-shaped trap in a channel-shaped slab geometry, both experimentally and numerically. When the trap is perfect, there are three time regimes: First, a 1D behavior before the depletion zone reaches the "end" of the trap; second, a 2D behavior after the depletion zone passes the "end" of the trap but does not yet reach the boundary of the reactor; third, a 1D behavior again, after the depletion zone well "recognizes" the shape of the reactor. We discussed the meaning of the two crossover times, in particular in some limiting cases. When the trap is imperfect, as is the case in the experiments, the behavior is the same as for the perfect trap during the second and third regimes but different in the first regime.

ACKNOWLEDGMENTS

Support from NSF DMR Grant No. 0455330 is gratefully acknowledged. H.T. acknowledges support by the Israel Science Foundation (Grant No. 1342/04).

[1] A. A. Ovchinnikov and Y. B. Zeldovich, Chem. Phys. **28**, 215 (1978).
[2] A. Blumen, J. Klafter, and G. Zumofen, Phys. Rev. B **28**, R6112 (1983).
[3] R. Kopelman, Science **241**, 1620 (1988).
[4] D. Ben-Avraham and S. Havlin, *Diffusion and Reactions in Fractal and Disordered Systems*, (Cambridge University Press, Cambridge, 2000).
[5] A. Lin, R. Kopelman, and P. Argyrakis, Phys. Rev. E **53**, 1502 (1996).
[6] P. Argyrakis, R. Kopelman, and K. Lindenberg, Chem. Phys. **177**, 693 (1993).
[7] A. L. Lin, R. Kopelman, and P. Argyrakis, Phys. Rev. E **54**, R5893 (1996).
[8] C. N. Reilley, Pure Appl. Chem. **18**, 137 (1968).
[9] A. T. Hubbard and F. C. Anson, Anal. Chem. **38**, 58 (1966).
[10] C. R. Christensen and F. C. Anson, Anal. Chem. **35**, 205 (1963).
[11] *Advances in Electrochemistry and Electrochemical Engineering*, edited by P. Delahay and C. Tobias (Wiley, New York, 1961–1984).
[12] *Electroanalytical Chemistry: A Series of Advances*, edited by A. J. Bard (Dekker, New York, 1970), Vol. 4.
[13] S. H. Park, H. Peng, S. Parus, H. Taitelbaum, and R. Kopelman, J. Phys. Chem. A **106**, 7586 (2002).
[14] S. H. Park, H. Peng, R. Kopelman, P. Argyrakis, and H. Taitelbaum, Phys. Rev. E **67**, 060103(R) (2003).
[15] H. Peng, S. H. Park, P. Argyrakis, H. Taitelbaum, and R. Kopelman, Phys. Rev. E **68**, 061102 (2003).
[16] S. H. Park, H. Peng, R. Kopelman, P. Argyrakis, and H. Taitelbaum, Phys. Rev. E **71**, 031107 (2005).
[17] G. H. Weiss, R. Kopelman, and S. Havlin, Phys. Rev. A **39**, R466 (1989).
[18] H. Taitelbaum, R. Kopelman, G. H. Weiss, and S. Havlin, Phys. Rev. A **41**, 3116 (1990).
[19] S. Redner and D. Ben-Avraham, J. Phys. A **23**, L1169 (1990).
[20] S. Havlin, H. Larralde, R. Kopelman, and G. H. Weiss, Physica A **169**, 337 (1990).
[21] H. Taitelbaum, Phys. Rev. A **43**, 6592 (1991).
[22] S. Havlin and D. Ben-Avraham, Adv. Phys. **36**, 695 (1987); **51**, 187 (2002).